2021

Demand Side Management and Battery Storage Utilization to Increase PV Self-consumption of a Modulating Heat Pump

Maria Pinamonti
Free University of Bolzano, Italy, maria.pinamonti@natec.unibz.it

Alessandro Prada
University of Trento

Paolo Baggio
University of Trento

Demand Side Management and Battery Storage Utilization to Increase PV Self-consumption of a Modulating Heat Pump

Maria PINAMONTI[1]*, Alessandro PRADA[2], Paolo BAGGIO[2]

[1]Free University of Bolzano, Faculty of Science and Technology,
Bolzano, Italy
maria.pinamonti@natec.unibz.it

[2]University of Trento, Department or Equivalent,
Trento, Italy

* Corresponding Author

ABSTRACT

The combination of photovoltaic (PV) systems and heat pumps for heating and cooling of buildings is a promising solution to increase the share of renewable energy in the residential sector. The interaction between the system components is fundamental to assure a high performance of the system. The level of PV energy self-consumption is strictly dependent on the control strategy applied to the system. The solar source is intermittent and it does not always match the building loads for heating and cooling.
Furthermore, even the heating and cooling demands are strongly time-dependent in high performance buildings. For these reasons, an efficient control system is essential to ensure the high performance. Several papers in the literature have proposed advanced control techniques based on the model predictive control (MPC). However, their implementation in residential buildings is often limited due to high device costs.
This paper proposes a rule-based control strategy for a modulating air-source heat pump coupled with a PV plant, which provide space heating, space cooling and domestic hot water in a residential building. The proposed control strategy can be easily implemented in residential buildings by using low-cost board shields. The heat pump is modulated and optimized depending on the instantaneous PV production, to maximize the direct use of solar energy onsite. When an overproduction of PV energy occurs, the heat pump operates to store the solar energy as thermal energy, exploiting thermal storage tanks and the building thermal capacitance (aka virtual battery). The heat pump is controlled by varying its compressor rotational speed. The compressor is regulated to operate at the maximum capacity level compatible with the supplied PV power. The control strategy is evaluated in combination with a electric storage system. The efficacy of the control strategy is assessed by means of dynamic energy simulations. The simulations are run for the whole year. A parametric analysis is carried out by considering different PV and battery size, to understand the impact of the system component size on the results.

1. INTRODUCTION

Around 40% of the European Union (EU) energy consumption is related to the building use. The total energy demand of buildings is around 192 Mtoe, which is divided in 79% related to space heating (SH), 15% to domestic hot water (DHW), and 6% to space cooling (SC). Additionally, the use of space cooling in residential buildings is reported to be increasing in the last decade, because of several factors such as higher required comfort levels, climate change and the resulting increase in external air temperature. As reported by Eurostat, only the 19% of the energy consumed for heating and cooling in the European countries comes from renewable energy sources (RES) (Eurostat, 2018). A larger use of renewable energy sources is one of the main challenges to decarbonize the building energy sector.
The use of heat pump units is one of the most valuable solutions to reduce the primary energy demand and to integrate RES in buildings. Specifically, the combination of photovoltaic systems and heat pumps for heating and cooling of buildings is a promising solution to increase the use of renewable energy produced on-site. However,

several factors, such as the time gap between the energy availability and the building loads, are a limit for the system to reach high levels of renewable energy self-consumption. Considering the strong time dependency of the solar source and the building demand, the control strategy applied to the system is fundamental to increase the level of PV self-consumption. The interaction between the system components is fundamental to assure a high performance level of the system. Load-control strategies exploit the ability of the building system devices to work during preset operation periods to match the energy demand and the production. These strategies are commonly defined as Demand Side Management (DSM), and they can be applied to a wide range of electric applications. Heat pumps are characterized by a great potential for load flexibility, hence they are a promising tool for DSM applications. The control strategies can be divided in two main categories, depending on their conceptual structure: rule based (RB) controls and model predictive controls (MPC). The first group can be implemented in the system with the use of simple low-cost controllers, while the second group involves more complex solutions that involve models for weather forecast and predictions about the building/system behavior. Several papers in the literature have shown the efficacy of advanced control techniques based on the MPC (Fischer and Madani, 2017; Péan, Salom and Costa-Castelló, 2019). However, their implementation in residential buildings is often limited due to high device costs.

RBC are designed to shape the electric load with non-predictive approaches. Different strategies can be implemented depending on the trigger parameters that are used to control the system. Arteconi et al. (Arteconi, Hewitt and Polonara, 2013) studied a control strategy to shift the heat pump operation out of the peak hours (from 16:00h to 19:00h). They found a benefit of shifting of the HP operation in terms of a reduction of the energy costs. Tatjewski et al. (Tatjewski *et al.*, 2016) designed a control algorithm to increase the performance of the HP, reaching an increase of the COP around 10%. Dentel and Betzold (Dentel and Betzold, 2017) proposed a control strategy based on the instantaneous PV production. The results showed an increase of self-consumption by 21%. RBC can be integrated with no additional costs into the controllers of modern HP units, which are already provided of internet connectivity. The efficacy of these solutions needs to be studied further, to better understand their potential in comparison to more sophisticated solutions (i.e. MPC). In most cases, the studies about MPC compared the results to a poorly design controller as a reference case. This assumption leads to an overestimation of the MPC benefits, and the potential of well-designed RBC can be analyzed more in detail (Fischer *et al.*, 2017).

This paper presents a RBC for a modulating air-source heat pump, which provide SH, SC and DHW for a residential building. The system is coupled with a rooftop PV system. The proposed control strategy can be easily implemented in residential buildings by using low-cost board shields The heat pump is modulated and optimized depending on the instantaneous PV production, to maximize the direct use of solar energy onsite. A similar system has been analyzed in a previous study (Pinamonti, Prada and Baggio, 2020), and the results showed the efficacy of the proposed control strategy to increase the level of self-consumption of the system, and to decrease the energy purchased from the grid. The results proved the efficacy of the control strategy under different boundary conditions. In this paper, the integration of a battery system is evaluated, to point out the effect of the control strategy over the optimal size of the electric storage. The efficacy of storing the PV energy using the thermal capacitance of the buildings is analyzed considering different battery storage sizes.

2. METHODS

This study proposes a control strategy to increase the PV self-consumption of a HP system in a residential building. The heat pump has a variable-speed compressor, and it works to provide space heating, space cooling and domestic hot water to the building. When an overproduction of PV energy occurs, the heat pump operates to store the solar energy as thermal energy, exploiting thermal storage tanks and the building thermal capacitance (aka virtual battery). The heat pump is controlled varying its compressor rotational speed. The compressor is regulated to operate at the maximum capacity level compatible with the supplied PV power. The efficacy of the control strategy is assessed by means of dynamic energy simulations. The simulations are run for 1 year.

2.1 Case study

The case study consists of a reference building located in Bolzano, northern Italy. The building is developed on two floors above ground, with a total net area of 140 m^2 and a ratio S/V of 0.59. The heated volume is divided into 4 thermal zones. The air change rate of the building is set to 0.5 ACH (European Committee for Standardization-CEN, 2017), and it is increased to 1.5 ACH during the summer period to represent the window opening by the users. The DHW demand is 186 l/day (UNI - Ente Italiano di Normazione, 2014). The DHW demand profile is defined as prescribed by the European Standards (European Committee for Standardization-CEN, 2016).

The building system consists of an air-source HP, which provides SH, SC and DHW. Two water tanks are integrated in the system, one dedicated to space heating and space cooling, the other one for DHW. The tanks are filled with water, with a volume of 250 liters (SH/SC tank) and 150 liters (DHW tank). The tanks are subjected to thermal stratification. The HP is controlled to maintain the temperature in the tanks at the set-point level, with priority to the DHW tank. The set-point for the DHW tank is set to 50 °C, while the SH/SC tank set-point varies following a outside temperature reset (OTR) curve. In heating mode, the set-point varies from 40°C to 20°C in relation to the outdoor air temperature going from -5°C ad 20°C respectively. For cooling mode, the set-point goes from 12°C to 20°C with the external air temperature varying from 35°C to 26°C. A radiant floor system is connected to the SH/SC tank, and a regulation system controls the water flows for the 4 zones separately. The indoor air temperature is maintained in between 20°C and 26°C ±1 °C. A rooftop PV plant is installed on the building toward South, with a slope of 45°. The nominal power of the system is around 3.20 kW. The heat pump is modeled as a variable-speed compressor unit, based on a performance map that describes the operating behavior of the unit. The performance map was defined starting from detailed steady-state measurements supplied by the manufacturer for a new generation heat pump. The independent variable for the HP model are the inlet air temperature, the outlet water temperature and the compressor speed (i.e. inverter frequency). The dependent variable are the heating rate capacity and the electric input of the compressor. The electric input (Y_{el}) is defined with a polynomial equation (Eq. 1) obtained from the manufacturer data for given sink and source temperatures.

$$Y_{el} = b_0 + b_1 \cdot {T_{cond,out}}^2 + b_2 \cdot T_{ev,in} + b_3 \cdot {T_{ev,in}}^2 \quad (1)$$

The compressor speed is regulated depending on the set-point temperature and the inlet flow temperature in the HP. For DHW production, the HP is working at its maximum capacity. To improve the HP working conditions, the heat pump model is regulate with a minimum stop and running time, and imposing a maximum frequency variation of the inverter of 5 Hz/min.

The proposed control strategy is implemented with a simple control algorithm. Its operation requires common-use sensors for temperature (external air, water flow, thermal storage) and power measurements (domestic appliances, heat pump consumption and photovoltaic production). The control strategy is based on the study presented by Pinamonti et al. (Pinamonti, Prada and Baggio, 2020).

The PV surplus ($P_{PV,production}$) is assessed excluding the appliances' electric load, as in Eq. 2.

$$P_{PV,surplus} = P_{PV,production} \cdot 0.9 - P_{appliances} \quad (2)$$

A reduction factor of 10% is applied to the $P_{PV,production}$ in the formula. The percentage of electric input ($Y_{el,\%,surplus}$) is defined as the ratio between the available PV surplus and the electric input (Yel) at the actual operating conditions of the heat pump calculated as in Eq. (19). The $Y_{el,\%,surplus}$ is calculated as in Eq. 3.

$$Y_{el,\%,surplus} = \frac{P_{PV,surplus}}{Y_{el}} \quad (3)$$

Then, this value is used to define the maximum frequency for the HP operation allowed by the PV availability, using Eq. 4.

$$f = -0.0042 \cdot {Y_{el,\%}}^2 + 1.3861 \cdot Y_{el,\%} - 1.3342 \quad (4)$$

This level of frequency is used in the model to control the heat pump operation during surplus periods.

The PV energy is stored by the system using 3 different solutions: by overheating (or overcooling during summer) the water tanks for SH/SC and DHW, by changing the indoor air temperature set-point by ±2 °C to exploit the building thermal mass as virtual battery, and by charging a Li-ion battery system. Two different strategies are proposed for the energy storage in the water tanks, considering the prioritization of the DHW tank over the SH/SC tank (CS1), and vice versa (CS2). For the battery storage, a battery size varying from 0 to 19.2 kWh is analyzed. The battery has a charging efficiency of 90% and the low limit for the fractional state of charge (FSOC) is set to 0.2. The regulator efficiency is set to 78%, and the inverter efficiency to 96%. Two different charging modes (CM) are proposed. In a first case, the HP is controlled as described above for CS1 and CS2, and any further PV overproduction is stored in the battery system. This charging mode is defined as CM1. In a second case (CM2), the PV surplus is sent with priority to the battery, and, when the battery is totally charged, the PV energy is used to

operate the HP following the different CSs. The battery charge is controlled through the fractional state of charge (FSOC).
The system operation is evaluated by means of the self-consumption ($SC_{\%}$) and the self-sufficiency ($SS_{\%}$), as in Eq. 5 and Eq. 6.

$$SC_{\%} = \frac{Self\ consumption}{PV\ production} \quad (5)$$

$$SS_{\%} = \frac{Self\ consumption}{Total\ loads} \quad (6)$$

The efficacy of the thermal and electric storage is assessed considering different combination of the proposed solutions. In particular, 3 main cases are analyzed:

- Battery storage only (CM1 and CM2);
- Battery storage + overheating of the water tanks (CS1 and CS2);
- Battery storage + overheating of the storage tanks + building thermal mass activation (CS1+ and CS2+).

3. RESULTS

The system performance is evaluated for the standard control strategies, and the proposed control strategies with different energy storage solutions (electric storage, thermal storage within the water tanks and within the building thermal inertia). The analysis is carried out using a dynamic energy simulation software. The simulations are run for 1 year, using a 1-minute time step.
In a first analysis, the proposed control strategies are combined with a battery system, considering an electric storage size varying from 1.2 to 19.2 kWh.
The self-consumption level of the system is analyzed with and without battery integration. The results related to the different control strategies and storage capacities are shown in Figure 1 for the CM1 and CM2.

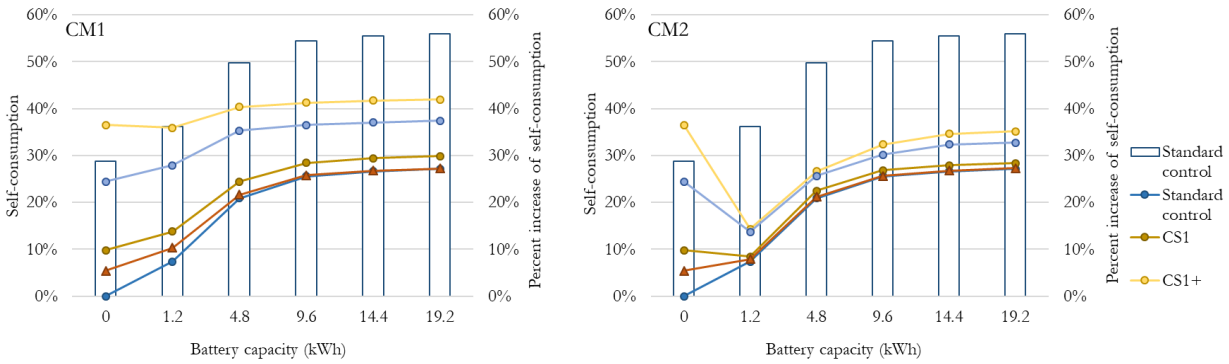

Figure 1 - Level of self-consumption (%) for the different control strategies in relation to the battery capacity (kWh) with the CM1 (left) and CM2 (right)

The first graph shows that, for the standard control strategy, a maximum increase of self-consumption of 27% is achievable with the largest battery capacity (19.2 kWh). In this case, increasing the battery size above 9.6 kWh leads to a minimal benefits to the self-consumption of the system. The increase of $SC_{\%}$ related to the battery integration is reduced for the system working with to the CSs characterized by higher levels of self-consumption. For instance, the application of CS1 leads to an increase of self-consumption of 37% without the battery integration. For the same control strategy, the maximum increase of $SC_{\%}$ related to the battery integration is limited to 5%. The second graph shows the results for the application of CM2. For all the cases, the self-consumption levels are reduced in comparison to CM1. Moreover, the impact of the battery integration leads to a reduction of self-consumption in relation to CS1+ and CS2+, for small battery sizes. For CS2+, the benefit of the thermal mass activation over the SC is compensate with a battery storage capacity of 4.8 kWh. A noticeable difference between the two charging modes

(CM1 and CM2) is that the impact of the storage sizes is reduced for the CSs with the highest levels of self-consumption in the case of CM1. For CM2, the battery size impacts the results until a capacity level around 9.6-14.4 kWh, depending on the control strategy.
Then, the annual amount of energy required from the grid for each solution is analyzed. The results are shown in Figure 2 for the CM1 and CM2.

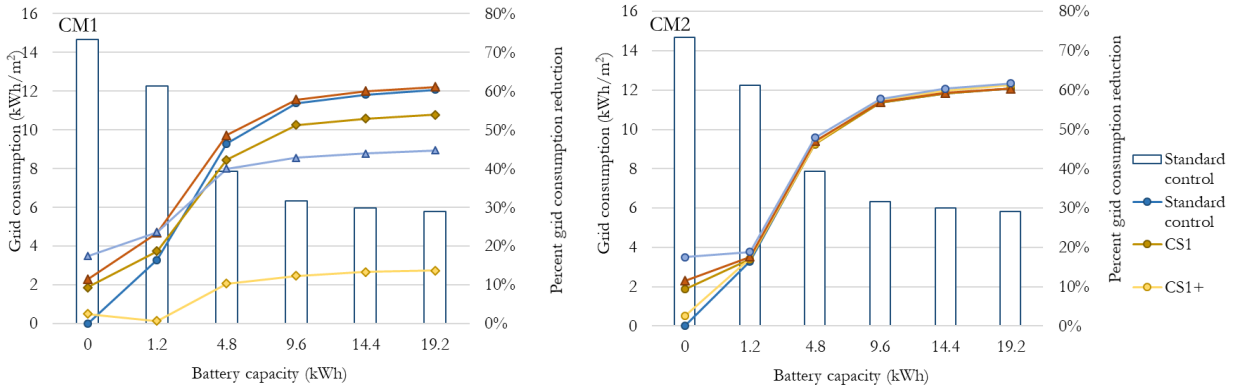

Figure 2 - Grid energy consumption (kWh/m^{2}y) in relation to the battery capacity for the standard control strategy and the percent consumption achievable with the application of the CS2 for different battery sizes with CM1 (left) and CM2 (right)

For CM1 with the standard control strategy, the maximum energy reduction level achievable with the battery integration is 60%. The control strategy CS1+, which leads to the highest level of self-consumption, is characterized by the lowest level of grid consumption reduction (14%). The highest level of energy reduction is achievable with the application of CS2 (61%), with a small increase in comparison to the standard control. The results for the standard control move towards the results of CS2 with increasing battery capacities. Contrarily to the results for the system without battery storage, CS2+ leads to a limited level of grid consumption reduction (45%) in this case. Considering the charging mode CM2, the impact of the different control strategies over the grid consumption is minimized in relation to the majority of the analyzed storage capacity levels. In this case, a slightly higher level of energy reduction is achievable with CS2+ (62%) in comparison to the other CSs. The grid reduction achievable with the CS2+ is only 2%, but an increase of self-consumption around 5% is achievable. It is worth noticing that similar levels of grid energy reduction can be achieved by applying the CS2+ or with the integration of 1.2 kWh electric storage capacity in the system with the standard control strategy. For the self-consumption level, a battery of 9.6 kWh is required with the standard control strategy to reach the same $SC_{\%}$ achievable with the CS2+.
Moreover, the impact of the battery integration over the grid demand magnitude is analyzed and the results are shown in Figure 3 and Figure 4.

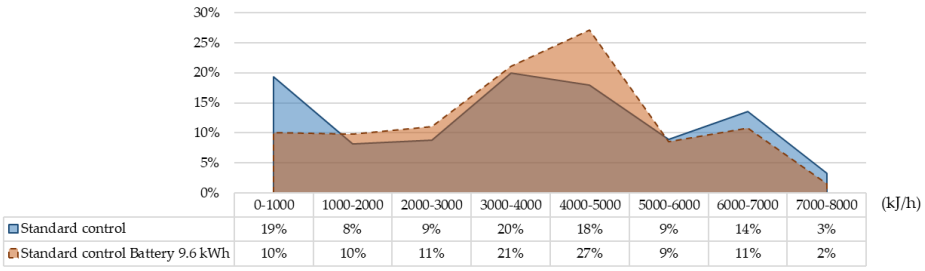

	0-1000	1000-2000	2000-3000	3000-4000	4000-5000	5000-6000	6000-7000	7000-8000
Standard control	19%	8%	9%	20%	18%	9%	14%	3%
Standard control Battery 9.6 kWh	10%	10%	11%	21%	27%	9%	11%	2%

Figure 3 - Frequency distribution of the grid demand magnitude (kJ/h) of the system throughout the year for the standard control with and without battery integration

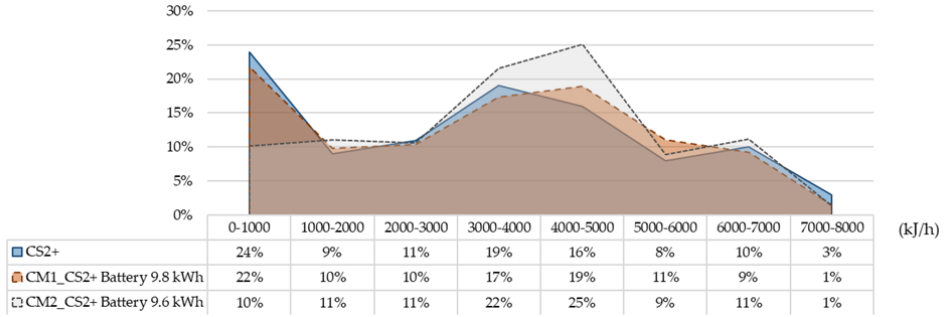

	0-1000	1000-2000	2000-3000	3000-4000	4000-5000	5000-6000	6000-7000	7000-8000
CS2+	24%	9%	11%	19%	16%	8%	10%	3%
CM1_CS2+ Battery 9.8 kWh	22%	10%	10%	17%	19%	11%	9%	1%
CM2_CS2+ Battery 9.6 kWh	10%	11%	11%	22%	25%	9%	11%	1%

Figure 4 - Frequency distribution of the grid demand magnitude (kJ/h) of the system throughout the year for the CS2+, with and without battery, considering the two charging modes CM1 and CM2

The first graph shows that the integration of the battery leads to an increase of the medium-magnitude grid withdrawals (+9%). At the same time, the use of the battery decreases the purchase of energy at low and high load levels (-9% and -3%). The second graph shows the distribution of the grid demand magnitude in combination with the CS2+ without battery, and with battery for the two charging modes CM1 and CM2. As shown before, the CS2+ alone is able to slightly reduce the demand peak load periods by 4%, increasing the frequency of smaller grid withdrawals. Similar results are found with the integration of the battery and selecting the CM1, with a slight reduction of low and high load peaks, and with a shift of the peak demand to slightly higher load levels (4000-5000 kJ/h). With the application of CM2, the results are similar to the standard control case. In this case, the battery integration leads to a decrease of low-load levels (-14%), but it does not significantly affect the high loads (-2%), which are already decreased by the application of the control strategy. The difference for the battery integration with and without control strategy is found in relation to a slight reduction of the medium- and high-load withdrawals (1-2%).

A parametric analysis is carried out by varying the PV size and the battery size. The size of the PV plant is defined by the number of panels. Starting from 12 (reference case), the number of PV panels is varied from 6 to 18. The results are analyzed in terms of grid consumption, self-consumption and self-sufficiency, as shown in Figure 5 and Figure 6. Considering the grid consumption (left column), the integration of the battery reduces the impact of the control strategies with increasing storage sizes as seen before. Specifically, when installing a battery size of 1.2 kWh, the control strategy is able to reduce the grid consumption up to 2.0 kWh/m^2, in case of charging mode CM1 and the building thermal mass activation with a 30-m^2 PV installation. Nonetheless, with the integration of a 1.2-kWh electric storage, the thermal mass activation (CS2+) shows higher grid consumption than the other solutions in combination with small PV areas. Considering larger battery sizes, the impact of the different control strategies is neutralized, with the exception of the CS2+ CM1 that shows higher grid consumption. This result shows the inability of this solution to exploit the battery storage. Looking at the self-consumption rate, the solution CS2+ with CM1 shows the highest level of self-consumption in all the analyzed cases. In all the cases, the thermal mass activation (CS2+ with both CM1 and CM2) is able to increase the self-consumption rate for every size of PV and battery. Moreover, the application of CS2+ with CM1 leads to higher levels of self-sufficiency with small battery size (1.2 kWh). With a battery storage of 4.8 kWh, CS2+ leads to higher level of self-sufficiency only in relation to large PV areas (20 m2). Considering battery sizes larger than 4.8 kWh, the solution that leads to the maximum level of self-sufficiency is CS2+ with CM2.

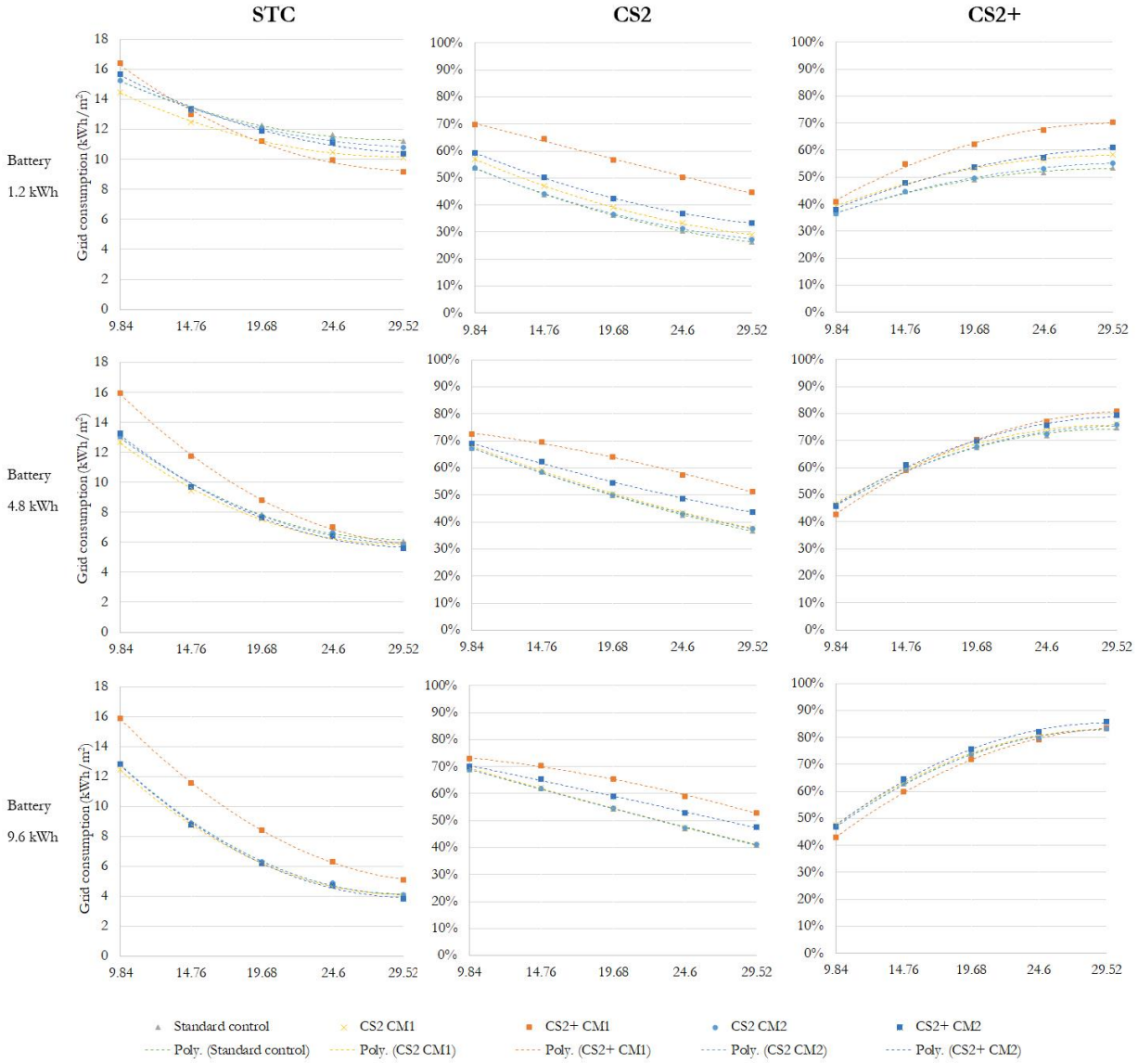

Figure 5 - Relation between the main performance indicators of the system (grid consumption, self-consumption, and self-sufficiency) and the PV area, considering different battery size (from 1.2 to 9.6 kWh) and control strategy

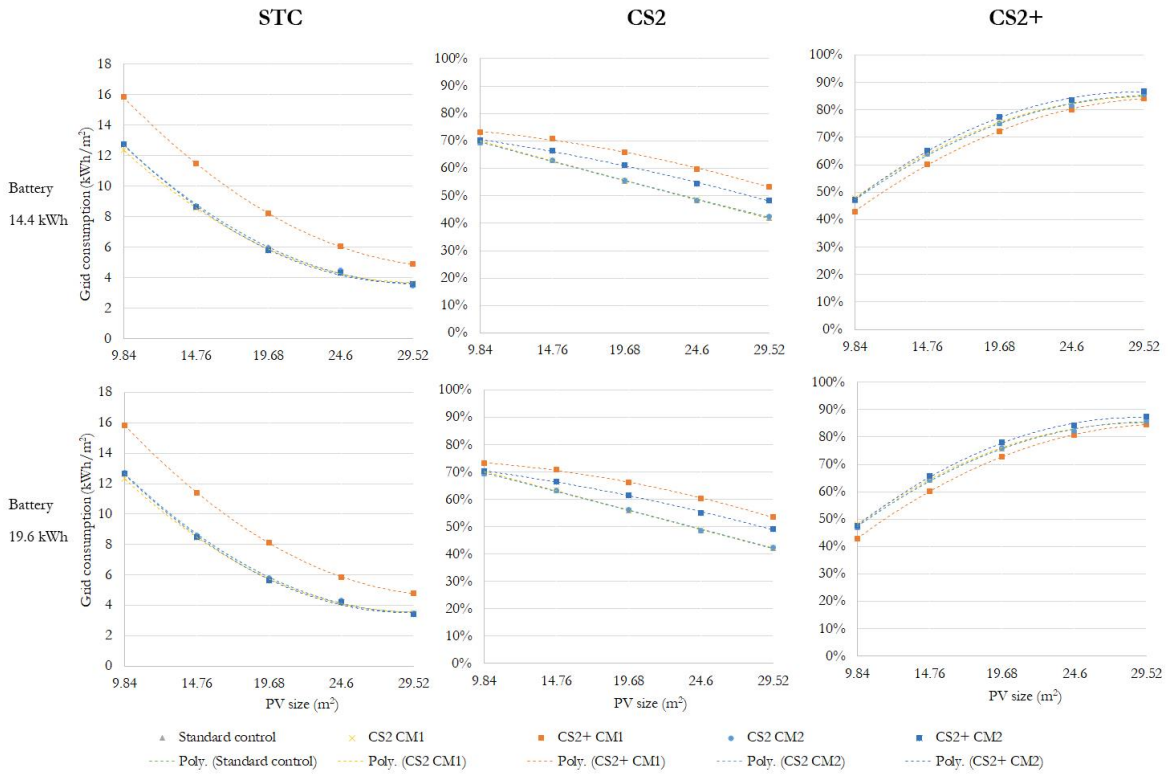

Figure 6 - Relation between the main performance indicator of the system (grid consumption, self-consumption, and self-sufficiency) and the PV area, considering different battery size (from 1.2 to 9.6 kWh) and control strategies

Lastly, the relation between the self-consumption and the grid consumption for different PV and battery sizes is shown in Figure 7. The best solutions are characterized by low grid consumption and high self-consumption levels (upper left part of the graph). The thermal mass activation (triangles) shows again its potential to increase the level of self-consumption while reducing the grid consumption.

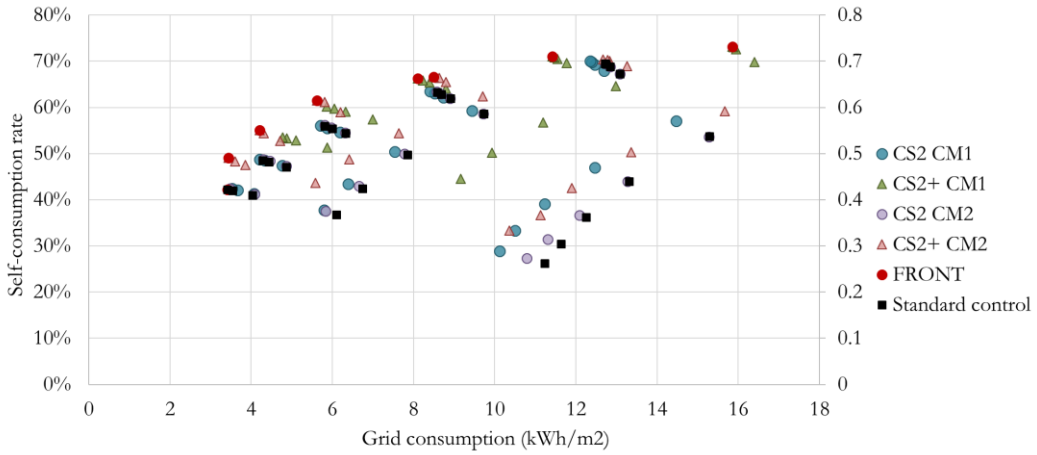

Figure 7 - Self-consumption and grid consumption relation for the different control strategies with battery integration and variable PV size, identification of the Pareto front

The graph shows the identification of the Pareto front, which identifies the solutions that are able to maximize the level of self-consumption.

4. CONCLUSIONS

This study shows the efficacy of a rule-based control strategy to increase the self-consumption of a PV and HP system for heating and cooling supplies, in combination with a an electric storage system. The results showed a constant increase of self-consumption in relation to different battery sizes. Nevertheless, considering the annual grid consumption, the benefits of the control strategy are neutralized with the integration of a battery storage larger than 1.2 kWh. Specifically, the application of the proposed CS2+ without battery and the installation of a 1.2 kWh reach similar results for the analyzed cases. A parametric analysis of the PV and battery size showed that, in combination to small battery size and large PV areas (30 m^2), the thermal mass activation (CS2+) is able to achieve a grid consumption reduction of 2.0 kWh/m^2. Nonetheless, with small PV areas, the same control strategy leads to an increase of grid consumption, in comparison to the other solutions. The thermal mass activation showed to be able to increase the self-consumption of the system for all the analyzed battery and PV sizes. Specifically, the increase of self-consumption increases with increasing PV areas.

NOMENCLATURE

CM	charging mode
CS	control strategy
DHW	domestic hot water
FSOC	fractional state of charge
HP	heat pump
MPC	model predictive control
RES	renewable energy source
SC	space cooling
$SC_{\%}$	self-consumption rate
SH	space heating
$SS_{\%}$	self-sufficiency rate
PV	photovoltaic

REFERENCES

Arteconi, A., Hewitt, N. J. and Polonara, F. (2013) 'Domestic demand-side management (DSM): Role of heat pumps and thermal energy storage (TES) systems', *Applied Thermal Engineering*. Elsevier Ltd, 51(1–2), pp. 155–165. doi: 10.1016/j.applthermaleng.2012.09.023.

Dentel, A. and Betzold, C. (2017) 'Control Strategies for Geothermal Heat Pump Systems in Combination with Thermal and Electrical Storage Units', in *Building Simulation*, pp. 292–298. doi: 10.26868/25222708.2017.081.

European Committee for Standardization-CEN (2016) 'EN12381-3 Energy performance of buildings - method for calculation of design heat load - Part 3: Domestic hot water systems heat load and characterisation of needs, Module M8-2, M8-3'.

European Committee for Standardization-CEN (2017) 'EN 12831-3 Energy Performance of buildings - method for calculation of the design heat load - Part 3: Domestic hot water systems heat load and characterisation of needs, Module M8-2, M8-3'.

Eurostat (2018) *Energy statistics - Share of energy from renewable energy sources*. Available at: https://ec.europa.eu/eurostat/data/database.

Fischer, D. *et al.* (2017) 'Comparison of control approaches for variable speed air source heat pumps considering time variable electricity prices and PV', *Applied Energy*. Elsevier Ltd, 204, pp. 93–105. doi: 10.1016/j.apenergy.2017.06.110.

Fischer, D. and Madani, H. (2017) 'On heat pumps in smart grids: A review', *Renewable and Sustainable Energy Reviews*, 70(October), pp. 342–357. doi: 10.1016/j.rser.2016.11.182.

Péan, T. Q., Salom, J. and Costa-Castelló, R. (2019) 'Review of control strategies for improving the energy flexibility provided by heat pump systems in buildings', *Journal of Process Control*. Elsevier Ltd, 74, pp. 35–49. doi: 10.1016/j.jprocont.2018.03.006.
Pinamonti, M., Prada, A. and Baggio, P. (2020) 'Rule-Based Control Strategy to Increase Photovoltaic Self-Consumption of a Modulating Heat Pump Using Water Storages and Building Mass Activation', *Energies*, 13(23), p. 6282. doi: 10.3390/en13236282.
Tatjewski, P. *et al.* (2016) 'Design and implementation of the air/water heat pump controller with increased coefficient of performance', in *21st International Conference on Methods and Models in Automation and Robotics, MMAR*. IEEE, pp. 959–964. doi: 10.1109/MMAR.2016.7575267.
UNI - Ente Italiano di Normazione (2014) 'Prestazioni energetiche degli edifici Parte 2 : Determinazione del fabbisogno di energia primaria e dei rendimenti per la climatizzazione invernale, per la produzione di acqua calda sanitaria, per la ventilazione e per l'illuminazione in edifici non resid'.